Original Article
Effects of miR-520b on migration and invasion of cervical cancer cells through negative regulation of SOS1

Xiao-Di Zhang, Qun-Feng Zhang, Jue Liu

Department of Obstetrics and Gynecology, The Second Affiliated Hospital of South China University, Hengyang 421001, P. R. China

Abstract: Objective: The current study was designed to verify the hypothesis that miR-520b inhibits migration and invasion of cervical cancer cells via targeting SOS1. Methods: Bioinformatic tools were adopted to predict miRNAs that might bind to SOS1. Next, miR-520b was selected. The targeting regulatory relationship between miR-520b and SOS1 was verified using luciferase reporter gene assays. Cervical cancer tissues, along with para-cancerous tissues, diagnosed from January 2016 to July 2018, were involved in the current experiment. H&E staining was applied to explore changes in the histopathologic structure. Immunohistochemical staining was adopted to determine SOS1 expression in cancer tissues and adjacent tissues. A cervical cancer cell line with the highest expression of SOS1 was selected for the following experiments. Subsequently, the cells were transfected with miR-520b mimics, miR-520b inhibitors, or SOS1 shRNA sequences. Moreover, qRT-PCR and Western blotting were used to quantify mRNA and protein expression levels of MMP-9, SNAIL, and OCT-4. Scratch healing experiments and Transwell assays were conducted to evaluate migration and invasion abilities, respectively. Results: Results obtained from bioinformatic tools demonstrated that miR-520b was predicted to target SOS1. The targeted relationship was confirmed by dual luciferase reporter assays. H&E staining results indicated that the arrangement of cervical cancer tissues was disordered. At the same time, cells in the cancer tissues were arranged in nest bulk. Cell structures in the para-cancerous tissues were clear and tightly packed. There was an obvious boundary between the cells and sub-mucosal tissues. Immunohistochemistry results demonstrated that SOS1 was highly expressed in cancer tissues, compared with para-cancerous tissues. *In vitro* experiments showed that, compared with the NC group, mRNA and protein expression levels of MMP-9, SNAIL, and OCT-4, as well as migration and invasion abilities, in the miR-520b mimic group and SOS1 shRNA group were significantly downregulated (all $P < 0.05$). Expression levels of MMP-9, SNAIL, and OCT-4, as well as migration and invasion abilities, were obviously enhanced in SiHa cell lines treated with miR-520b inhibitors. In addition, the effects of miR-520b inhibitors on SiHa could be reversed by SOS1 silencing. Conclusion: Results of the present study suggest that miR-520b can inhibit migration and invasion abilities of cervical cancer cells by targeting SOS1.

Keywords: miR-520b, SOS1, cervical carcinoma, migration, invasion

Introduction

Cervical cancer is a kind of common malignant tumor that threatens female health, worldwide, showing a younger trend [1, 2]. Despite multiple measures, including resections, radiotherapy, and chemotherapy, adopted in the treatment of cervical cancer, recurrent rates and mortality rates have remained high. The reason lies in the occurrence of invasion and metastasis [3, 4]. Gene targeting therapy has been more and more frequently applied for treatment of sever-

al kinds of tumors. Thus, it is important to discover new target genes of invasion and metastasis in cervical cancer [5, 6].

Son of seveness homolog 1 (SOS1) is a member of the SOS family [7]. Previous studies have demonstrated that SOS1 is involved in occurrence and progression of many kinds of cancer. It has been reported that SOS1 may promote tumor metastasis by forming a complex with EPS8 and ABI1 under the action of LPA [8]. SOS1 may also participate in tumor prolifera-

tion, metastasis, and immunity through activating NF-κB signaling pathways [9]. Accumulating evidence has confirmed that there exists relationship between SOS1 and reproductive system cancers. For example, one study revealed that the integrity of the SOS1/EPS8/ABI1 complex is an important determinant of metastasis of ovarian cancer [8]. Another report showed that SOS1 was overexpressed in prostate cancer epithelial cells [10]. The present study focuses on the role of SOS1 in cervical carcinoma. SOS1 was selected as the target gene of miR-520b, according to the bioinformatics method and previous research. Previous studies have discovered that miR-520b acts as a tumor suppressor in colorectal cancer and gliomas [11, 12]. However, the effects on cervical cancer remain largely unknown. Thus, a hypothesis was proposed for this study, suggesting that miR-520b could regulate the biological characteristics of cervical cancer cells by targeting SOS1.

Materials and methods

Ethic statements

All experiments were conducted in accordance with the Declaration of Helsinki. The study was approved by the Ethics Committee of the Second Affiliated Hospital of South China University (Hengyang, Hunan, China). All patients enrolled in the study provided informed consent documentation.

Bioinformatics prediction

SOS1 (Accession number: NM_005633.3) mRNA was acquired from NCBI (https://www.ncbi.nlm.nih.gov/). Afterward, microRNA.org (http://www.microrna.org/microrna/home.do), miRWalk3.0 (http://mirwalk.umm.uni-heidelberg.de/), RNA22 v2.0 (https://cm.jefferson.edu/rna22/), and miRNApath (http://lgmb.fmrp.usp.br/mirnapath/tools.php) were used to predicted miRNAs that might bind to SOS1. Subsequently, Venny2.1.0 (http://bioinfogp.cnb.csic.es/tools/venny/index.html) was adopted to screen the intersection.

Dual luciferase reporter gene assays

Dual luciferase reporter gene assays were used to verify targeting regulatory relationships between miR-520b and SOS1. Wild-type (WT) and

mutant (MUT) 3'UTR sequences were designed and synthesized by Beijing Genomics Institute (Beijing, China). Target segments were then inserted into pmirGLO (3577193, Promega, USA) vectors. Correctly identified sequences of the luciferase reporter plasmids, WT and MUT, were co-transfected with miR-520b mimics or NC mimics into 293T cells (CBP60441, Cobioer, China), in accordance with manufacturer instructions for Lipofectamine 3000 (L3000001, Thermo Fisher, USA). The medium was changed 4 hours after transfection. The cells were then cultured in an incubator with 5% CO_2 at 37°C for 48 hours. The cells were washed with PBS 3 times. Next, the Luciferase Reporter Gene Detection Kit (E2920, Promega, USA) and microplate reader (DXI800, Beckman, USA) were used to detect luciferase reporter gene activity. This experiment was repeated 3 times.

Cervical cancer tissue collection and cell culture

A total of 68 cases of patients diagnosed with cervical cancer, from January 2016 to July 2018, were included in the present study. The median age of the patients was 55 (34-71) years old. Staging of cervical cancer was determined according to FIGO classification criteria. Out of the above patients, 52 were at I-II and 16 were at III-IV. In terms of classification, 56 cases were squamous cell carcinoma, while 12 cases were adenocarcinoma. A total of 68 pairs of resected cervical cancer samples and paracancerous tissue samples (over 5 cm away from the cancer tissues) were collected. The collected tissues were cut into two pieces. One piece was fixed with 10% formalin for pathological observation, while another was preserved in liquid nitrogen and transferred to a -80°C refrigerator for subsequent experiments.

Human cervical epithelial cells (JK-CS0992, ATCC, USA) were cultured in a complete medium (xy-059, Shanghai Xin Yu Biotech Co., Ltd, China). Cervical squamous cell carcinoma cell lines, including Hela (CL0134, Fenghuishengwu, China), SiHa (CM-H070, Shanghai Gaining Biotechnology Co., Ltd. China), MS751 (FS-X0384, Shanghai Fusheng Industry Co., Ltd., China), and HCC94 (CM-H470, Shanghai Gaining Biotechnology Co., Ltd., China), were cultured in minimum Eagle's medium (MEM) comprised of 10% FBS and 1% P/S. The cells were then incu-

bated in conditions of saturated humidity at 37°C with 5% CO_2. The cells were passaged at a ratio of 1:2-1:6 when cell confluence reached 80%. The complete medium was replaced every 2-3 days.

Construction of gene silencing vectors

The coding sequence of SOS (Accession: NM_005633.3) was obtained from NCBI (https://www.ncbi.nlm.nih.gov/). The SOS1 shRNA sequence (5'-CACCGCAATAGCTGATGCCCAATCAC-GAATGATTGGGCATCAGCTATTGC-3') and negative control sequence (5'-AATTCAAAAACAAC-AAGATGAAGAGCACCAACTCGAGTTGGTGCTC-TTCATCTTGTTG-3') were designed using a BLOCK-iT™ RNAi designer. They were then synthesized by Invitrogen (USA). Subsequently, the pcDNA3.1-GFP plasmid (#70219, Addgene, USA) was digested with EcoR I and Hind III. It was then connected with the target gene fragment. The plasmid was transfected and amplified in DH5α (KL1001, Shanghai Kanglang Biotechnology Co., Ltd., China). The recombinant vector was extracted using the EasyPure Genomic DNA Kit (EE101-01, TRANSGENE BIO-TECH, China). After identification via agarose gel electrophoresis, the purified recombinant plasmid was preserved at -80°C.

Cell grouping and transfection

Western blotting was performed, screening the cell line with the highest protein expression of SOS1 for the following experiments. Cervical cancer cells were then divided into several groups, including the NC group (cells transfected with negative control sequence), miR-520b mimic group (cells transfected with miR-520b mimics), miR-520b inhibitor group (cells transfected with miR-520b inhibitors), SOS1 shRNA group (cells transfected with SOS1 shRNA sequences), and miR-520b inhibitor + SOS1 shRNA group (cells transfected with miR-520b inhibitors and SOS1 shRNA sequences).

Transfection method: Cells at the logarithmic phase were transfected using Lipofectamine 3000 (L3000001, Thermo Fisher, USA). Concrete operating procedures were as follows: Transfection was performed when cell confluence reached 70%-90%. Cell density was adjusted to 3×10^5/mL using Opti-MEM. The cells were then seeded to 24-well culture plates. Subsequently, 1.5 μL Lipofectamine

3000 was dissolved in 50 μL Opti-MEM (solution A) and 1 μg DNA (2 μg/μL) containing 50 μL. Opti-MEM was added with 2 μL P3000™. The two solutions were mixed at a ratio of 1:1 and incubated at room temperature for 5 minutes. Next, the DNA-liposome vector complexes were added into 24-well culture plates containing cervical cancer cells. They were slightly shaken, replacing the culture medium after 24-48 hours.

H&E staining

Pathological changes of cancer tissues and para-cancerous tissues were observed through application of H&E staining. Slice samples were first dried in an oven at 60°C for 1 hour, then dewaxed and hydrated with xylene I and II for 5-10 minutes, respectively. The sections were then dehydrated in ethanol (100%, 95%, 90%, 85%, and 80%) for 2 minutes for a total of 2 times. They were then washed in distilled water for 2 minutes. Next, the sections were stained with hematoxylin for 8-10 minutes and washed under tap water for 1-2 minutes. They were differentiated with 1% hydrochloric alcohol for 30 seconds and returned to blue under running water. Subsequently, the sections were stained in eosin for 2-3 minutes. They were then washed with tap water for 1-2 minutes and dehydrated again in ethanol (100%, 95%, 90%, 85%, and 80%) for 5 minutes two times. Next, the sections were cleared in xylene I and xylene II for 3-5 minutes and 5-10 minutes, then sealed off with neutral gum. Finally, the sections were observed using an optical microscope (BX40, Olympus, Japan) and photographed (10 × 40).

Immunohistochemistry

Slices of paraffin-embedded biopsies were produced and dried in an oven at 60°C for 1 hour. They were dewaxed and hydrated with xylene I and II for 5-10 minutes, respectively. The sections were dehydrated in ethanol (100%, 90%, 80%, 70%, 60%, 50%, and 30%) for 5 minutes. Next, the slices were treated with 0.3% H_2O_2 at room temperature for 10 minutes and immersed in 0.01 M citric acid buffer (pH 6.0). They were irradiated in a microwave oven for 10 minutes. The slices with were washed PBS for 5 minutes and sealed with bovine serum albumin for 20 minutes. After removing the excess liquid, the slices were then incubated with the

Table 1. Primer sequences

Gene	Forward primer (5'-3')	Reverse primer (5'-3')
SOS1	GAGTGAATCTGCATGTCGGTT	CTCTCATGTTTGGCTCCTACAC
MMP-9	TGGACGATGCCTGCAACGTG	GTCGTGCGTGTCCAAAGGCA
SNAIL	CCACTATGCCGCGCTCTTT	TCAGCGGGGACATCCTGAGCA
OCT-4	AGCAACTCCGATGGGGCTCC	GCCCCACATCGGCCTGTG
GAPDH	TGCACCACCAACTGCTTAGC	TCTTCTGGGTGGCAGTGATG

addition of rabbit polyclonal antibody SOS1 (1:1000, ab140621, ABCAM, UK) at 37°C for 1 hours. They were washed with PBS for 3 minutes a total of 3 times. The following day, the slices were incubated with the addition of rat anti-rabbit (IgG) secondary antibody (1 µg/mL, ab99697, ABCAM, UK) at 37°C for 20 minutes. They were then washed with PBS for 5 minutes a total of 3 times. The slice samples were then added with streptavidin-biotin complex and incubated at 37°C for 30 minutes. They were washed with PBS for 5 minutes a total of 3 times. They were stained with diaminobenzidine (DAB) and counter-stained using hematoxylin for 2 minutes. The sections were washed with running water and dehydrated it in ethanol. They were sealed off with neutral gum. Finally, the samples were observed under a microscope. Staining intensities (SI) and positive percentages (PP) of the samples were calculated. The SI score was divided into 4 grades: 0, 1, 2, and 3 representing colorless, light yellow, pale brown, and tan, respectively. The PP score was divided into 5 grades: Zero represents positive cells that were less than 5%; 1: Positive cells were 5%-25%; 2: Positive cells were 25%-50%; 3: Positive cells were 51%-75%; and 4: Positive cells were above 75%. The product of SI and PP was considered as the comprehensive score. Zero was considered as negative, 1 was marked as weakly positive (+), and 2 was regarded as moderately positive (++). When the comprehensive score was equal to or more than 3, the slices were regarded as strongly positive [13].

qRT-PCR

TRIzol Reagent (15596026, Invitrogen, USA) was utilized to extract the total RNA in cervical cancer cell lines. The RNA was diluted with ultrapure water treated by diethyl phosphorocyanidate (DEPC). RNA concentrations and quality levels were measured by comparing A260/280 ratios. Subsequently, the extracted RNA was reverse-transcribed into cDNA using the SuperScript IV First-Strand Synthesis System (1809-1200, Invitrogen, USA). The reaction system was as follows: 1 µg RNA template, 1 µL Oligo d (T20), 1 µL Ribonuclease inhibitor, 1 µL DTT, 1 µL dNTP mix, 4 µL SSIV buffer, and 20 µL DEPC-treated water. RT-qPCR was conducted using SYBR®Premix Ex TaqTM II reagent (HRR081B, Shanghai yihui Biological Technology Co., Ltd., China). GAPDH was used as an internal reference. Primers were designed and synthesized by Shenzhen BGI Health Technology Co., Ltd. (Shenzhen, China) (**Table 1**). The reaction system included: 12.5 µL SYBR®Premix Ex Taq^{TM} II (2x, 8.5 µL ddH$_2$O, 2 µL DNA Templates, 1µL PCR Forward Primer, 1 µL PCR Reverse Primer). Reaction conditions were as follows: Pre-denaturation at 95°C for 10 seconds, denaturation at 95°C for 5 seconds, and extension at 60°C for 20 seconds (40 cycles). Dissolution curves were used to verify the specificity and reliability of PCR results. Moreover, mRNA expression levels of related genes were calculated by $2^{-\Delta\Delta Ct}$. ΔCt = CT (target gene) - CT (GAPDH), $\Delta\Delta$Ct = ΔCt (experimental group) - ΔCt (control group). The experiment was repeated 3 times.

Western blotting

RIPA lysate was added to the PMSF. The final concentration of PMSF was 1 mM. Cervical cancer cells were washed with PBS 3 times, then added with RIPA lysate (5×10^6 cells were added with 1 mL RIPA lysate). Subsequently, the cells were incubated on ice and the lysates were centrifuged at 12,000 × g for 30 minutes. Protein concentrations were detected using a BCA kit (AR0146, Wuhan Boster Biological Technology Ltd., China). After separating via sodium dodecyl sulfate polyacrylamide gel electrophoresis (SDS-PAGE), the proteins were transferred onto PVDF membranes. Next, the membranes were blocked with tris buffered saline with Tween 20 (TBST) containing 5% bovine serum albumin for 1 hour. Next the blocking liquid was abandoned. Subsequently, the membranes were incubated with primary antibody SOS1 (1:1000, ab140621, ABCAM, UK), MMP-9 (1 µg/mL, ab73734, ABCAM, UK), SNAIL (2 µg/mL, ab53519, ABCAM, UK), OCT-4 (1 µg/mL, ab27985, ABCAM, UK), and GAPDH
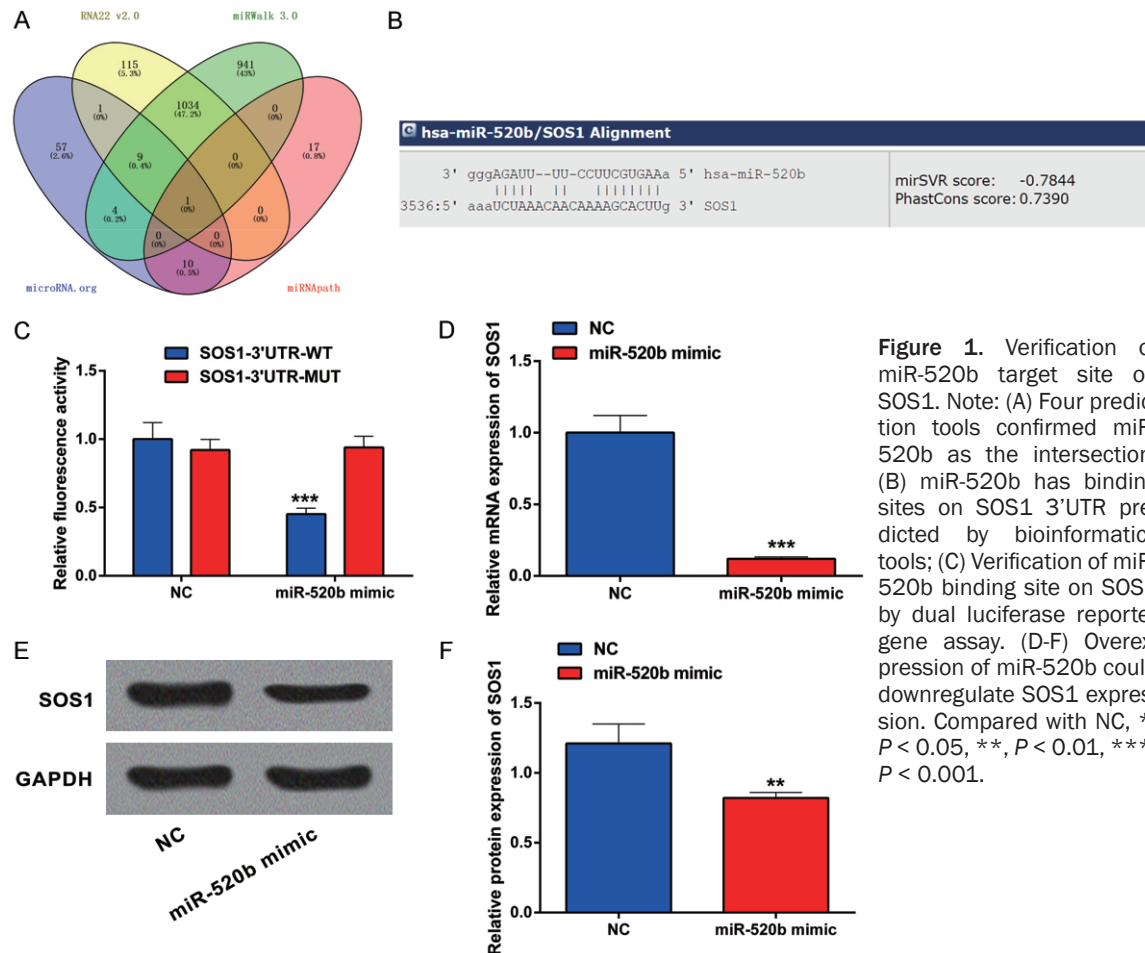
Figure 1. Verification of miR-520b target site on SOS1. Note: (A) Four prediction tools confirmed miR-520b as the intersection; (B) miR-520b has binding sites on SOS1 3'UTR predicted by bioinformatics tools; (C) Verification of miR-520b binding site on SOS1 by dual luciferase reporter gene assay. (D-F) Overexpression of miR-520b could downregulate SOS1 expression. Compared with NC, *, $P < 0.05$, **, $P < 0.01$, ***, $P < 0.001$.

(1:1000, ab8245, ABCAM, UK) and placed at 4°C overnight. The membranes were then washed with TBST for 30 minutes and added with second antibody IgG (1:2000, ab6721, ABCAM, UK). After culturing for 4-6 hours, the membranes were washed with PBST for 3 × 15 minutes. Chemiluminescence signals were detected using ECL (Pierce, Waltham, MA, USA). Target protein expression levels were quantified by determining the relative density of target protein bend to the internal reference (GAPDH). The experiment was repeated 3 times.

Scratch healing testing

Each well of the 6-well plate was seeded with 5 × 10^5 cells after transfecting for 48 hours. The next day, a sterile gun was used to draw a straight line on the cell surface under the guidance of the straight edge. The cells were then washed with PBS for 5 minutes for a total of 3 times. They were incubated with a serum-free medium. Each group of cells were photographed under an inverted microscope at 0 hours and 48 hours after culturing. Relative mobility was calculated using the following formula: (0 h scratch width - 48 h scratch width)/0 h scratch width × 100%. The experiment was independently repeated 3 times.

Transwell assays

Matrigel gel (356234, Beijing Think Far Technology Co., Ltd., China) was diluted with precooling serum-free DMEM medium at a ratio of 1:10. The Transwell upper chamber was then added with 100 μL diluted matrigel gel and incubated at 37°C for 4 hours. Next, 200 μL cell suspension (5 × 10^5/mL) was added to the Transwell upper chamber while the lower chamber was added with 600 μL DMEM medium.
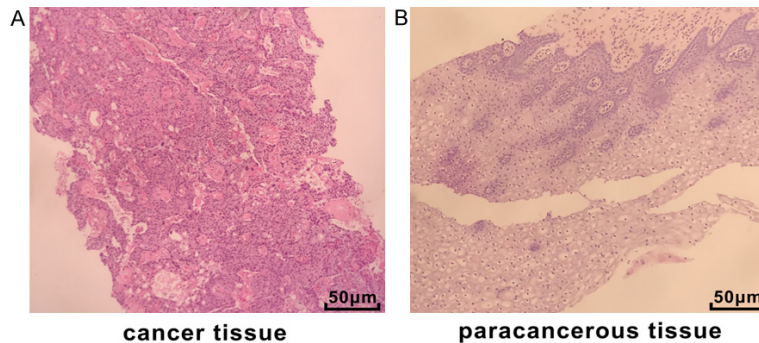
Figure 2. H&E staining results of cervical cancer and adjacent tissues (200×).
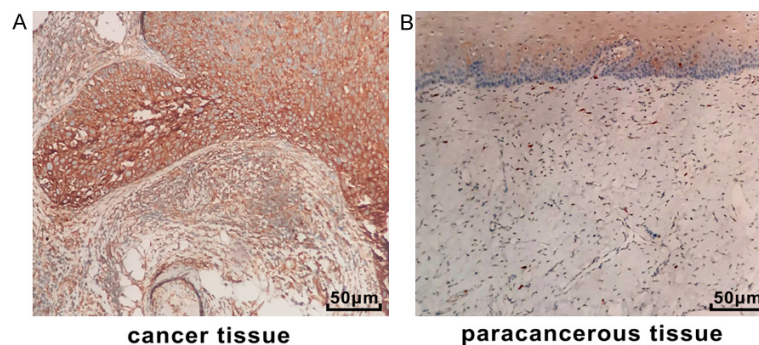

Figure 3. SOS1 expression in cervical cancer tissues and para-cancerous tissues detected using immunohistochemistry (400×).

After staining with 0.5% crystal violet for 15 minutes, in accordance with the introduction of Transwell (3413, Beijing Solarbio Science & Technology Co., Ltd., China), an inverted microscope (XDS-800D, Shanghai Caikon Optical Instrument Co., Ltd., China) was adopted to detect staining results. Three visual fields were randomly selected to calculate cells penetrating the Matrigel. The invasion rate was calculated using the following formula: cells penetrating the Matrigel/total number of cells × 100%. The experiment was repeated 3 times.

Statistical analysis

Statistical analysis was performed using SPSS 21.0 software. Experiment data are presented as mean ± standard deviation. Normal distribution and variance homogeneity were measured. Comparisons were performed using t-tests. Differences between multiple groups were compared via one-way analysis of variance (ANOVA). Post-hoc tests were also performed using Tukey's multiple comparisons in one-way ANOVA. Non-normal distributions of measurement data were compared using Kruskal-Wallis

tests. $P < 0.05$ indicates statistical significance.

Results

Bioinformatics prediction results

RNA22 v2.0, miRWalk 3.0, microRNA.org, and miRNA-path were used to predict miRNA that might have binding sites on SOS1 and 82, 1160, and 1989. A total of 28 miRNAs were selected, respectively. Interestingly, it was found that miR-520b was the intersection of these miRNAs predicted according to the above four prediction software systems (**Figure 1A**). Accumulating evidence has indicated that miR-520b plays a cancer suppressor role in many kinds of cancer A previous study indicated that overexpression of miR-520b could inhibit the invasion and metastasis of colorectal cancer cells [11]. In addition, another study reported that miR-520b could inhibit the growth and proliferation of glioma cells [12]. Another report confirmed that miR-520b overexpression could induce proliferation of ovarian cancer cells [14]. However, few studies have revealed the effects of miR-520b on cervical cancer cells. The present study confirmed that miR-520b has binding sites with SOS1 3'UTR, according to dual luciferase reporter assays. At the same time, qRT-PCR and Western blotting experiments indicated that miR-520b could downregulate SOS1 expression (**Figure 1B-F**). Thus, whether miR-520b could affect the invasion and metastasis of cervical cancer cells by targeting SOS1 will be explored in the following experiments.

H&E staining results

H&E staining was utilized to detect the histopathological characteristics of cancer tissues and para-cancerous tissues. Results indicated that (**Figure 2**) cervical cancer specimens were arranged in nest bulk. The nuclear were of different sizes. Deep stained, thickened karyotheca, and pathologic mitosis could be seen. In

Table 2. SOS1 expression in cervical cancer tissues and para-cancerous tissues

	SOS1 expression				P
	Negative (-)	Weakly positive (+)	Medium positive (++)	Strong positive (+++)	
adjacent tissue	14	35	16	3	0.0079
Gastric tissue	3	23	25	17	
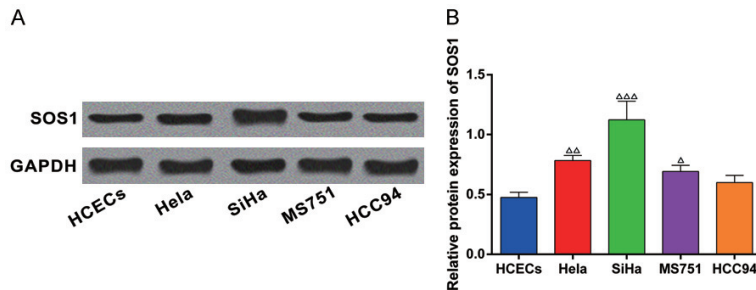
Figure 4. SOS1 protein expression in different cervical cancer cell lines. Note: (A) Protein band of SOS1 in different cervical cancer cell lines; (B) Quantification of SOS1 protein expression in different cervical cancer cell lines. Compared with HCECs, Δ, $P < 0.05$, ΔΔ, $P < 0.01$, ΔΔΔ, $P < 0.001$.

adjacent tissues, cell structures were clear and complete tightly packed. The intercellular space could be obviously observed. There was also a clear boundary between adjacent tissues and submucosal tissues.

Immunohistochemical staining results

Immunohistochemistry was utilized to detect SOS1 expression in cervical cancer and adjacent tissues. Results revealed that (**Figure 3**; **Table 2**) an uneven expression existed in the cytoplasm and nucleus, compared with para-cancerous tissues. Moreover, positive SOS1 expression was upregulated in cancer tissues ($P < 0.05$).

The highest expression level of SOS1 was found in SiHa cell lines

Western blotting was adopted to screen cervical cancer cell lines with the highest expression of SOS1. Results indicated that (**Figure 4**), compared with HCECs, SOS1 protein expression was upregulated in Hela, SiHa, and MS751 (all $P < 0.05$). Moreover, SiHa cells showed the highest expression of SOS1. Thus, the SiHa cell line was selected for subsequent experiments.

miR-520b inhibited the migration ability of SiHa through targeting SOS1

SiHa cell lines were treated with miR-520b mimics, miR-520b inhibitors, or SOS1 shRNA. Scratch healing experimentation was then per-

formed to detect the migration ability in each group. Results indicated that (**Figure 5**), compared with the NC group, the scratch healing rate in the miR-520b mimic group and SOS1 shRNA group was significantly downregulated, while that in the miR-520b inhibitor group was obviously upregulated (all $P < 0.05$). Furthermore, the migration ability of SiHa induced by miR-520b inhibitors could be reversed by SOS1 shRNA.

miR-520b inhibited the invasive ability of SiHa through targeting SOS1

SiHa cell lines were treated with miR-520b mimics, miR-520b inhibitors, or SOS1 shRNA. Transwell assays were then performed to detect the invasion ability in each group. Results demonstrated that (**Figure 6**), compared with the NC group, migration rates in the miR-520b mimic group and SOS1 shRNA group were significantly reduced. The migration ability of cervical cancer cells in the miR-520b inhibitor group was highly induced (all $P < 0.05$). At the same time, the invasive ability of SiHa induced by miR-520b inhibitors could be reversed by SOS1 shRNA.

Western blotting and qRT-PCR were adopted to determine mRNA and protein expression levels of MMP-9, SNAIL, and OCT-4 in each group. Results showed that (**Figure 7**), compared with the NC group, MMP-9, SNAIL, and OCT-4 mRNA and protein expression levels were obviously decreased in the miR-520b mimic group and SOS1 shRNA group. However, the above indexes were all increased when cells were treated with miR-520b inhibitors (all $P < 0.05$). SOS1 silencing could partly reverse expression of MMP-9, SNAIL, and OCT-4 induced by miR-520b inhibitors.

Discussion

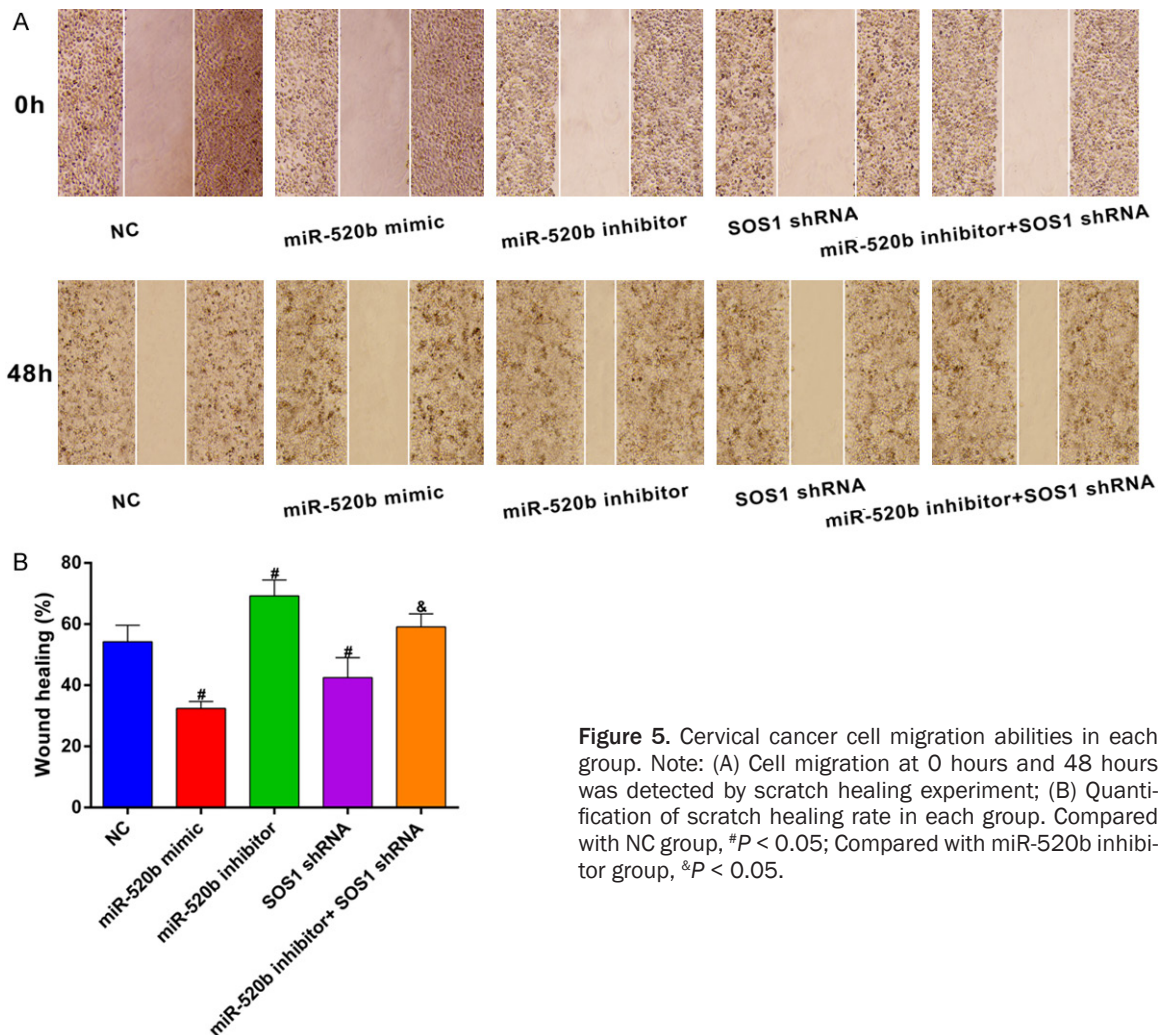Cancer is difficult to cure for a variety of reasons. One reason is invasion and metastasis

Figure 5. Cervical cancer cell migration abilities in each group. Note: (A) Cell migration at 0 hours and 48 hours was detected by scratch healing experiment; (B) Quantification of scratch healing rate in each group. Compared with NC group, #$P < 0.05$; Compared with miR-520b inhibitor group, &$P < 0.05$.

[15, 16]. Cervical carcinoma is one of the major diseases threatening the health of women, worldwide. It is important to reveal its development and progression mechanisms, aiming to improve curative effects of patients. From the perspective of biological characteristics of cervical cancer cells, the present study revealed the effects of miR-520b in regulating migration and invasion of cervical cancer cells through targeting SOS1.

A previous study showed that SOS1 was associated with morbidity of various kinds of cancer and that it could activate proto oncogene Ras [17]. Evidence demonstrated that SOS1/Ras signaling pathways are important targets in the treatment of metastatic cancer [18, 19]. In addition, research on reproductive system cancer has shown that expression of SOS1 was significantly upregulated in prostate cancer epi-

thelial cells [10]. Another study revealed that SOS1 and Ras protein may be involved in the development of epithelial ovarian cancer. High expression of SOS1 and Ras was shown to be related to shorter progression-free survival of patients [20]. Results obtained from immuno-histochemistry staining showed that, compared with para-cancerous tissues, SOS1 expression was significantly upregulated in cervical cancer tissues. This indicates that SOS1 might participate in the development of cervical carcinoma. The current study found that SOS1 has binding sites on miR-520b, according to the bioinformatics method. According to previous studies, miR-520b is a tumor suppressor in colorectal cancer and gliomas [11, 12]. The targeting regulatory relationship between miR-520b and SOS1 was confirmed by the dual luciferase reporter gene assay system. Subsequently, qRT-PCR and Western blotting were performed.
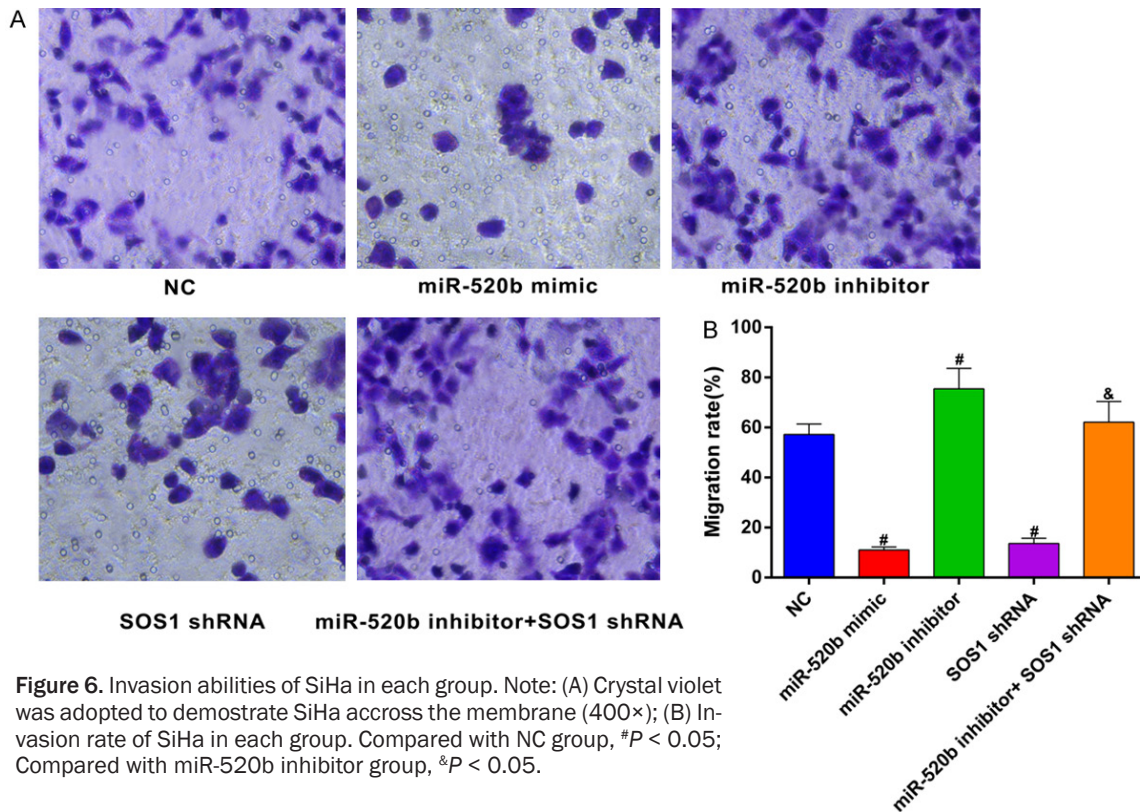
Figure 6. Invasion abilities of SiHa in each group. Note: (A) Crystal violet was adopted to demostrate SiHa accross the membrane (400×); (B) Invasion rate of SiHa in each group. Compared with NC group, #P < 0.05; Compared with miR-520b inhibitor group, &P < 0.05.
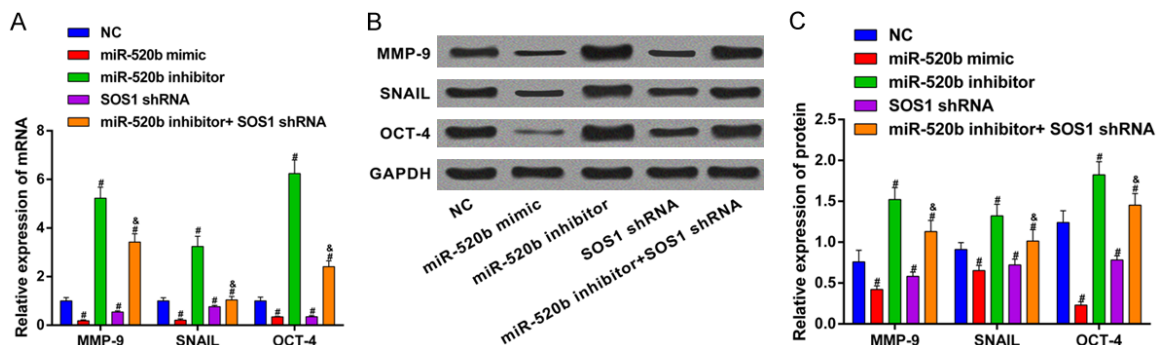

Figure 7. MMP-9, SNAIL, and OCT-4 mRNA and protein expression of SiHa in each group. Note: (A) mRNA expression of MMP-9, SNAIL, and OCT-4 in each group; (B) Protein bands of MMP-9, SNAIL, and OCT-4 in each group; (C) Quantification of protein expression of MMP-9, SNAIL, and OCT-4. Compared with NC group, #P < 0.05; Compared with miR-520b inhibitor group, &P < 0.05.

Results indicated that miR-520b could inhibit expression of SOS1.

SiHa cell lines, with the highest expression of SOS1, were selected for the subsequent experiments. Results of scratch healing experimentation indicated that miR-520b overexpression or SOS1 silencing could inhibit the migration ability of SiHa. Results obtained from Transwell assays showed that overexpression of miR-520b or SOS1 silencing could inhibit invasion

abilities of SiHa. At the same time, silencing of SOS1 could reverse the induction of invasion in SiHa by miR-520b inhibitors. Matrix metalloproteinase-9 (MMP-9) is a member of Matrix metalloproteinases (MMPs). According to recent research, MMP-9 was overexpressed in multiple cancers and associated with the infiltration and development of carcinoma [21, 22]. High expression of SNAIL protein showed an obviously positive correlation with grading and staging of tumors. It can also promote tumorigene-

sis and development [23, 24]. A clinical study showed that overexpression of SNAIL was closely related to high aggressiveness and poor prognosis of cancer [25, 26]. OCT4 is a member of the POU family of transcription factors. It is mainly expressed in embryonic stem cells. Accumulating evidence has indicated that it could participate in maintaining the infinite proliferative capacity of cells [27]. Other evidence has demonstrated that OCT4 overexpression could induce the malignant ability and growth of tumors [28, 29]. The current study found that miR-520b overexpression or SOS1 inhibition could inhibit expression of MMP-9, SNAIL, and OCT4, indicating that miR-520b overexpression or SOS1 inhibition could reduce the malignant degree of cancer.

In conclusion, the present study illustrated that miR-520b could inhibit migration and invasion of cervical cancer cells through targeting SOS1. Present results may explain the molecular mechanisms of cervical carcinoma, providing effective experimental evidence and therapy methods in cervical carcinoma. However, whether this study was affected by downstream pathways of miR-520b/SOS1 requires further investigation.

Disclosure of conflict of interest

None.

Address correspondence to: Jue Liu, Department of Obstetrics and Gynecology, The Second Affiliated Hospital of South China University, No. 35 Jiefang Avenue, Zhengxiang District, Hengyang 421001, P. R. China. Tel: +86-0734-8899694; E-mail: jueliu-0734@163.com

References

[1] Integrated genomic and molecular characterization of cervical cancer. Nature 2017; 543: 378-384.

[2] Small W Jr, Bacon MA, Bajaj A, Chuang LT, Fisher BJ, Harkenrider MM, Jhingran A, Kitchener HC, Mileshkin LR, Viswanathan AN and Gaffney DK. Cervical cancer: a global health crisis. Cancer 2017; 123: 2404-2412.

[3] Shi C and Zhang Z. MicroRNA-362 is downregulated in cervical cancer and inhibits cell proliferation, migration and invasion by directly targeting SIX1. Oncol Rep 2017; 37: 501-509.

[4] Zhang Z, Wang J, Li J, Wang X and Song W. MicroRNA-150 promotes cell proliferation, migration, and invasion of cervical cancer through targeting PDCD4. Biomed Pharmacother 2018; 97: 511-517.

[5] Wang Z, He S, Guo P, Guo X and Zheng J. MicroRNA-1297 inhibits metastasis and epithelial-mesenchymal transition by targeting AEG-1 in cervical cancer. Oncol Rep 2017; 38: 3121-3129.

[6] Zhou Y, An Q, Guo RX, Qiao YH, Li LX, Zhang XY and Zhao XL. miR424-5p functions as an anti-oncogene in cervical cancer cell growth by targeting KDM5B via the Notch signaling pathway. Life Sci 2017; 171: 9-15.

[7] Schlessinger J. How receptor tyrosine kinases activate Ras. Trends Biochem Sci 1993; 18: 273-275.

[8] Chen H, Wu X, Pan ZK and Huang S. Integrity of SOS1/EPS8/ABI1 tri-complex determines ovarian cancer metastasis. Cancer Res 2010; 70: 9979-9990.

[9] De S, Dermawan JK and Stark GR. EGF receptor uses SOS1 to drive constitutive activation of NFkappaB in cancer cells. Proc Natl Acad Sci U S A 2014; 111: 11721-11726.

[10] Timofeeva OA, Zhang X, Ressom HW, Varghese RS, Kallakury BV, Wang K, Ji Y, Cheema A, Jung M, Brown ML, Rhim JS and Dritschilo A. Enhanced expression of SOS1 is detected in prostate cancer epithelial cells from African-American men. Int J Oncol 2009; 35: 751-760.

[11] Xiao J, Li G, Zhou J, Wang S, Liu D, Shu G and Ren F. MicroRNA-520b functions as a tumor suppressor in colorectal cancer by inhibiting Defective in Cullin Neddylation 1 Domain Containing 1 (DCUN1D1). Oncol Res 2018; 26: 593-604.

[12] Cui S, Liu L, Wan T, Jiang L, Shi Y and Luo L. MiR-520b inhibits the development of glioma by directly targeting MBD2. Am J Cancer Res 2017; 7: 1528-1539.

[13] Konno R, Yamakawa H, Utsunomiya H, Ito K, Sato S and Yajima A. Expression of survivin and Bcl-2 in the normal human endometrium. Mol Hum Reprod 2000; 6: 529-534.

[14] Guan R, Cai S, Sun M and Xu M. Upregulation of miR-520b promotes ovarian cancer growth. Oncol Lett 2017; 14: 3155-3161.

[15] Wang J, Feng Y, Chen X, Du Z, Jiang S, Ma S and Zou W. SH3BP1-induced Rac-Wave2 pathway activation regulates cervical cancer cell migration, invasion, and chemoresistance to cisplatin. J Cell Biochem 2018; 119: 1733-1745.

[16] Xu H, Yuan Y, Wu W, Zhou M, Jiang Q, Niu L, Ji J, Liu N, Zhang L and Wang X. Hypoxia stimulates invasion and migration of human cervical cancer cell lines HeLa/SiHa through the Rab11 trafficking of integrin alphavbeta3/FAK/PI3K

pathway-mediated Rac1 activation. J Biosci 2017; 42: 491-499.

[17] Abbott JR, Hodges TR, Daniels RN, Patel PA, Kennedy JP, Howes JE, Akan DT, Burns MC, Sai J, Sobolik T, Beesetty Y, Lee T, Rossanese OW, Phan J, Waterson AG and Fesik SW. Discovery of aminopiperidine indoles that activate the guanine nucleotide exchange factor SOS1 and modulate RAS signaling. J Med Chem 2018; 61: 6002-6017.

[18] Singh A, Greninger P, Rhodes D, Koopman L, Violette S, Bardeesy N and Settleman J. A gene expression signature associated with "K-Ras addiction" reveals regulators of EMT and tumor cell survival. Cancer Cell 2009; 15: 489-500.

[19] Collins MA, Brisset JC, Zhang Y, Bednar F, Pierre J, Heist KA, Galban CJ, Galban S and di Magliano MP. Metastatic pancreatic cancer is dependent on oncogenic Kras in mice. PLoS One 2012; 7: e49707.

[20] Xiao ZH, Linghu H and Liu QF. Expressions of Ras and Sos1 in epithelial ovarian cancer tissues and their clinical significance. Nan Fang Yi Ke Da Xue Xue Bao 2016; 36: 1502-1507.

[21] Huang CF, Teng YH, Lu FJ, Hsu WH, Lin CL, Hung CC, Tung JN, Hsieh YH and Liu CJ. Beta-mangostin suppresses human hepatocellular carcinoma cell invasion through inhibition of MMP-2 and MMP-9 expression and activating the ERK and JNK pathways. Environ Toxicol 2017; 32: 2360-2370.

[22] Liao CL, Chu YL, Lin HY, Chen CY, Hsu MJ, Liu KC, Lai KC, Huang AC and Chung JG. Bisdemethoxycurcumin suppresses migration and invasion of human cervical cancer hela cells via inhibition of NF-kB, MMP-2 and -9 pathways. Anticancer Res 2018; 38: 3989-3997.

[23] Ito K, Park SH, Nayak A, Byerly JH and Irie HY. PTK6 inhibition suppresses metastases of triple-negative breast cancer via SNAIL-Dependent E-Cadherin regulation. Cancer Res 2016; 76: 4406-4417.

[24] Miao L, Yang L, Li R, Rodrigues DN, Crespo M, Hsieh JT, Tilley WD, de Bono J, Selth LA and Raj GV. Disrupting androgen receptor signaling induces snail-mediated epithelial-mesenchymal plasticity in prostate cancer. Cancer Res 2017; 77: 3101-3112.

[25] Alba-Castellon L, Olivera-Salguero R, Mestre-Farrera A, Pena R, Herrera M, Bonilla F, Casal JI, Baulida J, Pena C and Garcia de Herreros A. Snail1-dependent activation of cancer-associated fibroblast controls epithelial tumor cell invasion and metastasis. Cancer Res 2016; 76: 6205-6217.

[26] Taki M, Abiko K, Baba T, Hamanishi J, Yamaguchi K, Murakami R, Yamanoi K, Horikawa N, Hosoe Y, Nakamura E, Sugiyama A, Mandai M, Konishi I and Matsumura N. Snail promotes ovarian cancer progression by recruiting myeloid-derived suppressor cells via CXCR2 ligand upregulation. Nat Commun 2018; 9: 1685.

[27] Yong X, Tang B, Xiao YF, Xie R, Qin Y, Luo G, Hu CJ, Dong H and Yang SM. Helicobacter pylori upregulates Nanog and Oct4 via Wnt/beta-catenin signaling pathway to promote cancer stem cell-like properties in human gastric cancer. Cancer Lett 2016; 374: 292-303.

[28] Villodre ES, Kipper FC, Pereira MB and Lenz G. Roles of OCT4 in tumorigenesis, cancer therapy resistance and prognosis. Cancer Treat Rev 2016; 51: 1-9.

[29] Dong P, Xiong Y, Yu J, Chen L, Tao T, Yi S, Hanley SJB, Yue J, Watari H and Sakuragi N. Control of PD-L1 expression by miR-140/142/340/383 and oncogenic activation of the OCT4-miR-18a pathway in cervical cancer. Oncogene 2018; 37: 5257-5268.